Biochemical and Biophysical Research Communications 447 (2014) 70–76

Contents lists available at ScienceDirect

Biochemical and Biophysical Research Communications

journal homepage: www.elsevier.com/locate/ybbrc

Unusual binding mode of scorpion toxin BmKTX onto potassium channels relies on its distribution of acidic residues

Zongyun Chen [a,c,1], Youtian Hu [a,1], Jun Hu [a,1], Weishan Yang [a], Jean-Marc Sabatier [d], Michel De Waard [e,f,g], Zhijian Cao [a], Wenxin Li [a,c], Song Han [a,b,*], Yingliang Wu [a,c,*]

[a] State Key Laboratory of Virology, College of Life Sciences, Wuhan University, Wuhan 430072, China
[b] School of Basic Medical Sciences, Wuhan University, Wuhan 430071, China
[c] Center for Biodrug Research, Wuhan University, Wuhan 430072, China
[d] Inserm U1097, Parc Scientifique et Technologique de Luminy, 163, avenue de Luminy, 13288 Marseille Cedex 09, France
[e] Inserm U836, Grenoble Neuroscience Institute, Labex Ion Channels Science and Therapeutics, 38042 Grenoble Cedex 09, France
[f] Université Joseph Fourier, Grenoble, France
[g] Smartox Biotechnology, avenue du Grand Sablon, 38700 La Tronche, France

ARTICLE INFO

Article history:
Received 15 March 2014
Available online 3 April 2014

Keywords:
Scorpion toxin BmKTX
Acidic residues
Potassium channels
BmKTX-D33H analog
Binding mode
Electrostatic repulsion

ABSTRACT

Besides classical scorpion toxin–potassium channel binding modes, novel modes remain unknown. Here, we report a novel binding mode of native toxin BmKTX towards Kv1.3 channel. The combined experimental and computational data indicated that BmKTX-D33H analog used the classical anti-parallel β-sheet domain as the channel-interacting interface together with the conserved channel pore-blocking Lys^{26}. However, the wild-type BmKTX was found to use Arg^{23} rather than Lys^{26} as the new pore-blocking residue, and mainly adopt the turn motif between the α-helix and antiparallel β-sheet domains to recognize $K_v1.3$ channel. Together, these findings not only reveal that scorpion toxin–potassium channel interaction modes are more diverse than thought, but also highlight the functional role of toxin acidic residues in mediating diverse toxin–potassium channel binding modes.

1. Introduction

Venomous scorpions are known as "living fossils" since they maintained an ancient anatomy and are adapted to survive extreme climate changes over the past 400 million years [1]. For their survival, scorpions have developed efficient venoms for prey capture and their defense against predators [2]. Because of evolutionary selection pressure, scorpion toxins acting on potassium channels have arisen from a great variety of primary structures, and most of them exhibit similar 3D structures containing one α-helix and one anti-parallel β-sheet [3,4]. So far, two well-known interacting modes have been identified between toxins and potassium channels: One uses the anti-parallel β-sheet domain to recognize potassium channels [5–9]. This is the case of toxins like ChTX, AgTX2, MTX and ADWX-1. The second one uses the α-helical domain to bind potassium channels [10,11]. Classically, toxins such as P05, ScyTx and BmP05 use this mode of interaction. Although extensive proteomic and transcriptomic analyses of animal venoms lead to the discovery of an ever increasing number of novel toxin amino acid sequences [12], it still remains unclear whether scorpion toxins are really forced to use these two described modes of interaction with potassium channels.

Lately, we demonstrated that electrostatic interactions between scorpion toxins and potassium channels play a dominant role in defining the mode of interaction. We were able to convert BmP05 binding interface (the α-helical domain) towards nonbinding interface and vice versa by simply translocating its negatively charged residues from the β-sheet non-binding interface into the α-helix binding interface. The resulting BmP05-T mutant was then found to use the anti-parallel β-sheet domain as the novel binding interface [13]. Such a switch between the two classical interacting modes indicated that toxin acidic residues play important roles in orienting the toxin blocking face that will interact with potassium channels. In order to further investigate and understand the role of acidic residues on toxin binding modes, a native 37-residue scorpion toxin BmKTX that possesses two acidic interestingly-located residues (Asp^{19} and Asp^{33}) was selected for this study [14]. Structural analyses illustrate that Asp^{33} is spatially adjacent to the highly conserved Lys^{26} residue with a contact distance of ~5 Å in

* Corresponding authors at: State Key Laboratory of Virology, College of Life Sciences, Wuhan University, Wuhan, China. Fax: +86 (0) 27 68752146.
E-mail addresses: Hansong@whu.edu.cn (S. Han), ylwu@whu.edu.cn (Y. Wu).
[1] These authors contributed equally to the work.

http://dx.doi.org/10.1016/j.bbrc.2014.03.101
0006-291X/

the anti-parallel β-sheet domain of BmKTX structure (Protein Databank (PDB) code: 1BKT) [15]. In the homologous scorpion toxins ChTX, AgTX2 and ADWX-1, the same lysine residue (Lys^{27} or Lys^{26} depending of the toxin concerned) is the one that physically occludes the pore of potassium channels [5–7] (block by the anti-parallel β-sheet domain). Here, the adjacency between Asp^{33} and Lys^{26} in BmKTX was found to impede the side chain of Lys^{26} to block the potassium channel pore because of the strong electrostatic repulsion between Asp^{33} and the acidic residues in the outer vestibule of potassium channels. Therefore, this particular scorpion toxin adopts the turn motif between the α-helix and the antiparallel β-sheet domain to recognize $K_v1.3$ channel together with Arg^{23} as the new pore-blocking residue. To the best of our knowledge, this unique binding mode adopted by the scorpion toxin BmKTX towards potassium channels can now be considered as the third ever described interaction mode existing among structurally similar scorpion toxins. Our findings therefore enrich the diversity of modes of scorpion toxin-potassium channel interactions, and further highlight the functional role of toxin acidic residues in defining the functional binding mode adopted by toxins.

2. Materials and methods

2.1. Toxin site-directed mutagenesis

BmKTX was generated by overlapping PCR and inserted into pGEX-6P-1 to produce the pGEX-6P-1-BmKTX expression vector. The QuickChange Site-Directed Mutagenesis Kit (Stratagene, U.S.A.) was used to produce BmKTX mutants based on the wild-type pGEX-6P-1-BmKTX plasmid. All plasmids were verified by DNA sequencing before expression.

2.2. BmKTX peptides and potassium channels

Wild-type BmKTX and its mutated analogs were produced according to a procedure described previously [6]. After transformed into *Escherichia coli* Rosetta (DE3) cells, cells were cultured at 37 °C in LB medium with ampicillin (100 μg/mL). When cell density reached about OD = 0.6, 0.5 mM isopropyl thio-b-D-galactoside (IPTG) was added to induce the expression at 28 °C. Cells were harvested after 4 h and resuspended in 50 mM Tris–HCl/(pH 8.0)/10 mM Na_2EDTA. Supernatant from the bacterial cell lysate was loaded to a GST-bind column. The purified fusion protein was then desalted by using centrifugal filter (Millipore, USA), and cleaved by enterokinase (Biowisdom, China) at 25 °C for 16 h. Protein samples were then separated by HPLC on a C18 column (10 × 250 mm, 5 μm) (Elite-HPLC, China) using a linear gradient from 10% to 80% acetonitrile with 0.1% TFA in 60 min, with detection at 230 nm. Peptides were eluted as major peaks at 20–25% acetonitrile. The molecular masses of the purified peptides were obtained by MALDI-TOF-MS (Voyager-DESTR, Applied Biosystems). The cDNAs encoding mouse $K_v1.3$ was subcloned into the *Xho* I/*Bam* HI sites of pIRES2-EGFP, a bicistronic expression vector (Clontech, USA) for coexpression with enhanced GFP.

2.3. Determination, molecular modeling, and analyses of BmKTX analogs and $K_v1.3$ channel

The secondary structures of wild-type BmKTX and its mutants were experimentally measured by Circular Dichroism (CD) spectroscopy. The 3D structure of mouse $K_v1.3$ channel was modeled using the KcsA channel (PDB code: 1BL8). The solution structure of BmKTX was retrieved from the PDB (code 1BKT). The BmKTX analogs were modeled using wild-type BmKTX as template through the SWISS-MODEL server (http://swissmodel.expasy.org/) as described previously [6].

2.4. Electrophysiological recordings

Electrophysiological experiments were carried out using the patch-clamp whole-cell recording mode as described previously [6]. HEK293 cells were transfected with appropriate cDNA plasmids using SofastTM Transfection Reagent (Sunma). Potassium currents were recorded 1–3 days after transfection and cell culture and positive cells were selected based on the presence of GFP fluorescence. Electrophysiological experiments were carried out at 22 ~ 25 °C using the patch-clamp whole-cell recording mode. Cells were bathed with mammalian Ringer's solution: 5 mM KCl, 140 mM NaCl, 10 mM HEPES, 2 mM CaCl2, 1 mM MgCl2, 10 mM D-Glucose, pH 7.4 with NaOH. A multichannel micro perfusion system MPS-2 (INBIO Inc, Wuhan, China) was used to exchange the external recording bath solution. The pipette solution contained: 140 mM KCl, 1 mM MgCl2, 1 mM EGTA, 1 mM Na2ATP, 5 mM HEPES (pH 7.4 with NaOH). The channel currents were elicited by depolarizing voltage steps of 200 ms from the holding potential −80 mV to +50 mV. Membrane currents were measured with an EPC10 patch clamp amplifier (HEKA Elekt-ronik, Lambrecht, Germany) interfaced to a computer running acquisition and analysis software (Pulse).

Data analyses were performed with IgorPro (WaveMetrics, Lake Oswego, OR), and IC_{50} values were deduced by fitting a modified Hill equation to the data: $I_{toxin}/I_{control} = 1/1 + ([\text{toxin peptide}]/IC_{50})$, where I is the peak current to the normalized data points obtained with at least five different toxin peptide concentrations. Results are mostly shown as mean ± S.E, n being the number of experiments.

2.5. Computer-aided molecular simulations of peptide–$K_v1.3$ channel interactions

The molecular simulation method was used to study the molecular mechanism of BmKTX and BmKTX-D33H peptides interacting with $K_v1.3$ channel. The ZDOCK program was used to generate the candidate complex structures [16], and AMBER 8 package was used to obtain the stable complex structures for the structural analysis as described previously [17].

3. Results

3.1. Spatial vicinity between the conserved Lys^{26} and Asp^{33} in BmKTX

The native 37-residue scorpion toxin BmKTX is a potent blocker of $K_v1.3$ potassium channel with an IC_{50} value of about 0.2 nM [14]. It folds along a classical 3D structure with one α-helix and one anti-parallel β-sheet (PDB code: 1BKT) [15]. Structurally, one acidic residue, Asp^{19}, locates in the α-helical domain, the other acidic, Asp^{33}, together with the conserved Lys^{26}, is located in the anti-parallel β-sheet domain in the C-terminal part of the toxin (Fig. 1). There is a distance of about 5.0 Å between the two Cα atoms of Asp^{33} and the conserved Lys^{26} residues. In some conformations of BmKTX structure, the Lys^{26} Nζ atom to Asp^{33} Od2 atom distance is less than 4.0 Å (Fig. 1B). Such a close distance more than likely impedes the side chain of the conserved Lys^{26} to block the channel pore because of the existence of strong electrostatic repulsion forces between Asp^{33} and the acidic residues of the outer vestibule of the $K_v1.3$ channel [13]. Therefore, the functional role played by Lys^{26} in BmKTX would be different from the conserved pore-blocking residues of other related toxins: Lys^{26} in ADWX-1 and Lys^{27} in ChTX (Fig. 1) [5,6]. In order to further understand the effect of

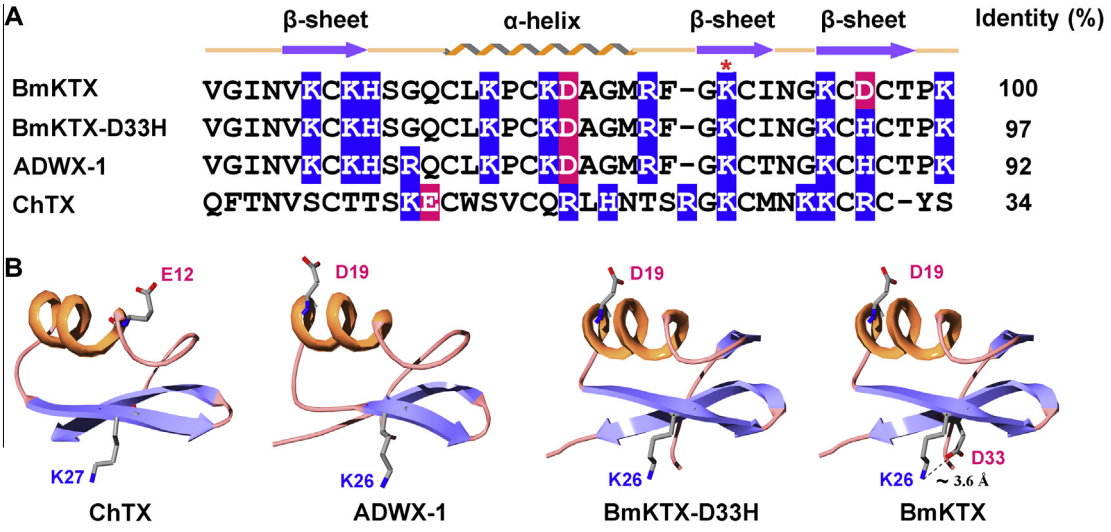

C

Toxin	Target	Structural Fold	Binding Interface	Pore-blocking Residue	IC_{50} (Pore-blocking residue mutant)/ IC_{50}(wt) Lys-Ala	Lys-Asn	Lys-Met	Reference
ChTX	Shaker	CSα/β	β-sheet	Lys27	-	>1000	>1000	19
AgTX2	Shaker	CSα/β	β-sheet	Lys27	686	-	-	20
ADWX-1	Kv1.3	CSα/β	β-sheet	Lys26	512	>1000	-	6
MTX	Kv1.2	CSα/β	β-sheet	Lys23	>1000	-	-	21
MTX	IKCa	CSα/β	β-sheet	Lys23	>1000	-	-	21

Fig. 1. Scorpion toxin BmKTX and BmKTX-D33H with the different distribution of their acidic residues. (A) Amino acid sequences of wild-type BmKTX, BmKTX-D33H, ADWX-1 and ChTX. (B) 3D structures of toxin ChTX (PDB code: 2CRD), ADWX-1 (PDB code: 2K4U), BmKTX-D33H and BmKTX (PDB code: 1BKT). The acidic residues and conserved Lys26 or Lys27 as the potential or known potassium channel pore-blocking residues were shown. In a conformation of BmKTX structure, the distance of Lys^{26} Nζ atom to Asp^{33} Od2 atom is about 3.6 Å. (C) Functional importance of the conserved pore-blocking residue of scorpion toxins with classical CSα/β fold, – means no tested data.

Asp^{33} on the binding mode of BmKTX on potassium channels, a highly similar BmKTX-D33H mutant was designed by replacing Asp^{33} by histidine, a conserved residue in the subfamily of BmKTX toxins [18] (Fig. 1). Recombinant BmKTX and BmKTX-D33H were successfully prepared as shown in Fig. 2 by respecting a previously published preparation procedure of the homologous ADWX-1 peptide [6].

3.2. Asp^{33} inhibits the channel blocking ability of Lys^{26} in BmKTX

Evaluation of the pore-blocking function of the conserved Lysine residue is the yardstick to judge whether BmKTX adopts the anti-parallel β-sheet domain to recognize potassium channel, which has been widely used in other structurally similar scorpion toxins with CSα/β fold (Fig. 1) [5,6,19–21]. The effect of Asp^{33} on Lys^{26} function in BmKTX was investigated by the following experiments. Firstly, we tested the binding affinities of BmKTX and BmKTX-D33H toxins on $K_v1.3$ channel. Despite the differences in the acidic residue distribution, both BmKTX and BmKTX-D33H efficiently blocked $K_v1.3$ currents with IC_{50} values of 90.5 ± 33.5 pM and 15.4 ± 8.6 pM, respectively (Fig. 3A–C and F). These results indicated that BmKTX-D33H remained a potent toxin blocker prompting us to further investigate the possibly novel role of Lys^{26}. Secondly, mutagenesis experiments were carried out to study the function of the conserved Lys^{26} in BmKTX. Four mutations were engineered (BmKTX-K26A, BmKTX-K26N, BmKTX-D33H/K26A and BmKTX-D33H/K26N). Three of them were successfully produced with the exception of BmKTX-K26A. Their CD spectra showed structural similarities with wild-type BmKTX (Fig. 3E), suggesting the conservation of the same 3D structures. As shown in Fig. 3B and F 1 nM BmKTX-K26 N could inhibit about 37.4% of $K_v1.3$ channel currents. The corresponding IC_{50} value was 5457.9 ± 1491.1 pM, which represents a mild 60-fold decrease in inhibitory affinity compared to the wild-type BmKTX toxin. In contrast to BmKTX-K26N, the activity of BmKTX-D33H/K26N mutant exhibited significantly greater drop in affinity for $K_v1.3$ channels (over 698-fold, from 15.4 ± 8.6 pM to 10741.2 ± 6992.3 pM) (Fig. 3G). Interestingly, the same observation was made for the conserved Lys^{26} on the binding affinity of similar peptide ADWX-1 (BmKTX-D33H/R11A/I28T). In the absence of Asp^{33}, mutation of Lys^{26} of ADWX-1 to Ala or Asn induced a significant drop in binding affinity of about 512-fold or over 1000-fold (unpublished data), respectively (Fig. 1) [6]. Altogether, these significant functional differences of the conserved Lys^{26} between BmKTX and the two double mutants that contain His^{33} suggest that Lys^{26} does not act as a channel pore-blocking residue in the presence of the spatially adjacent Asp^{33} in BmKTX.

3.3. Novel interacting face of BmKTX as a consequence of the presence of Asp^{33}

The non-classical function of the conserved Lys^{26} (due to the presence of Asp^{33}) suggests that BmKTX blocks $K_v1.3$ through another interface. To investigate this issue, we probed the effects of peptide alanine-scanning mutagenesis on the $K_v1.3$ blocking efficacies of BmKTX and its BmKTX-D33H analog. The CD spectra

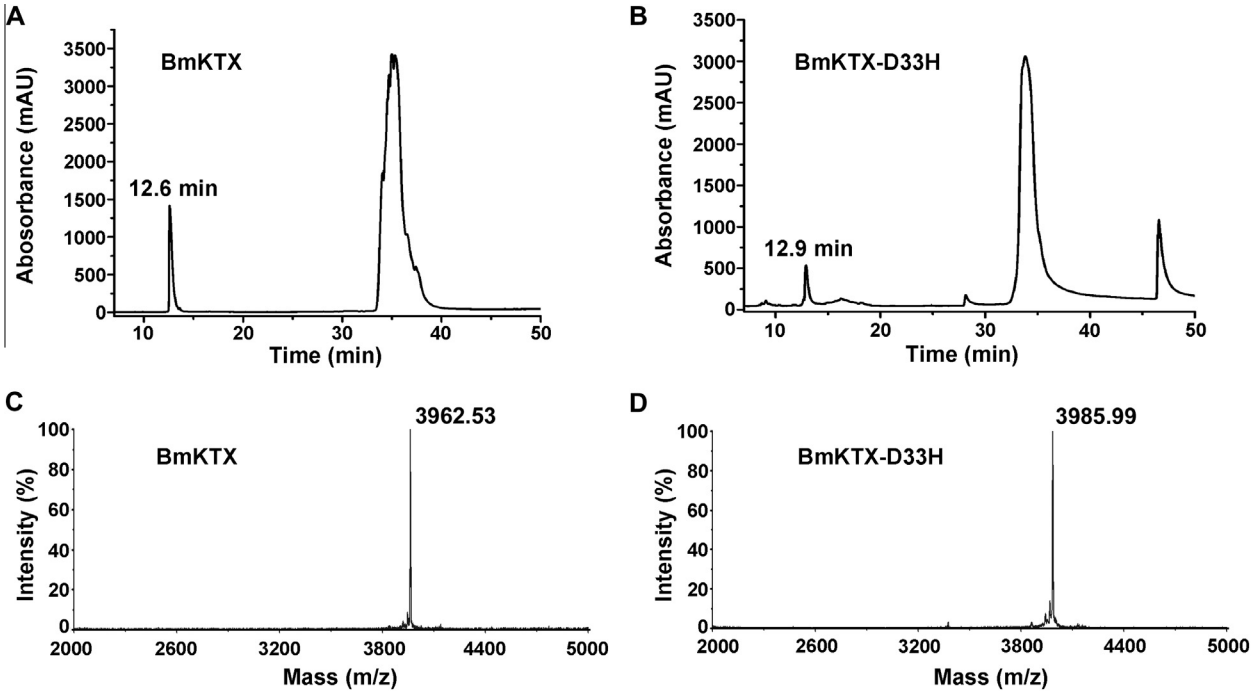

Fig. 2. Purification and mass spectra of scorpion toxin BmKTX and BmKTX-D33H. (A) Purification of BmKTX by using an HPLC system equipped with a C18 reversed-phase column. (B) Purification of BmKTX-D33H by HPLC on a C18 column. The HPLC fractions that contain each peptide are indicated by their peak elution times. (C) Mass spectrum of BmKTX. The experimental mass value is 3962.53 Da (the deduced value is 3962.78 Da). (D) Mass spectrum of BmKTX-D33H. The experimental value is 3985.99 Da (the deduced value is 3984.83 Da).

of these additional peptides also indicated their structural similarity with BmKTX (Fig. S1). In agreement with our hypothesis, mutating Asp^{33} resulted in marked differences in the identity of BmKTX functional amino acid residues that are critical for blocking the $K_v1.3$ channel (Table 1). Although for both BmKTX and BmKTX-D33H, Arg^{23} residue was particularly important for their pharmacology. However, noticeable differences pharmacological effects exist in other key residues, which suggest that BmKTX and BmKTX-D33H adopt different binding interfaces interacting with $K_v1.3$ channel. Among all tested amino acid positions, key functional BmKTX amino acid residues included only Arg^{23} and Phe^{24} since their replacements by alanyl produced severe affinity drops for $K_v1.3$ by 1940-, and 107-fold, respectively (Table 1). Among them, only one residue Arg^{23} was most important, indicating its unique functional role in BmKTX–Kv1.3 interaction. In contrast to BmKTX, BmKTX-D33H used the 'classical' binding interface that involved the β-strands in its C-terminal region. As such, it used a similar binding interface with ADWX-1, a toxin that shares a common acidic residue Asp^{19} with BmKTX-D33H [6]. Alanine substitution of Arg^{23}, Phe^{24}, Asn^{29} and Lys^{26} residue dramatically altered BmKTX-D33H blocking efficacy towards $K_v1.3$ currents 1770-, 1366-, 401-fold and 296-fold, respectively (Table 2), and among them, two residues Arg^{23}, Phe^{24} were most important, which is similar with ADWX-1 peptide and widely different from BmKTX peptide.

Based on these observations, we confirm our suspicion that the presence of Asp^{33} led to a novel BmKTX binding interface to block $K_v1.3$ currents. Remarkably, this change in binding interface occurs in spite of the very high sequence identity between BmKTX and BmKTX-D33H analog.

3.4. The unique BmKTX–$K_v1.3$ channel interaction mode is induced by the presence of Asp^{33}

To further illustrate the functional role of Asp^{33} in defining the mode of interaction of BmKTX with $K_v1.3$, we modeled BmKTX and BmKTX-D33H in complex with $K_v1.3$ channels by protein docking and molecular dynamic simulations according to methods that we have widely used before [6,8–11]. In agreement with our experimental data, the modeled complexes illustrated that the functionally important residues of BmKTX and BmKTX-D33H analog were also those that interacted with the $K_v1.3$ channels (Fig. 4). While some peptide residues that were important for toxin interaction with the channel were shared by BmKTX and BmKTX-D33H peptides, there were also obvious differences that could be supported from the spatial orientations and pore-blocking residues of each peptide in their docked positions onto $K_v1.3$ channels.

In the presence of Asp^{33}, BmKTX adopted an unprecedented binding mode towards $K_v1.3$ channel. Indeed, the turn motif between the α-helix and the antiparallel β-sheet domain was used as the channel-interacting interface (Fig. 4A). In the BmKTX–$K_v1.3$ channel complex, Arg^{23} was identified as the most critical residue for blocking $K_v1.3$ channel pore. It forms remarkable polar interactions with the conserved residues of the ion selectivity filter within the distance of 4 Å (Fig. 4B). These strong interactions between the toxin Arg^{23} residue and channel residues were well in line with the most significant effect of Arg^{23} on BmKTX binding affinity (Table 1). Phe^{24}, an important residue, was adjacent to the pore-blocking Arg^{23} residue, located near the selectivity filter of $K_v1.3$ channel. Structural analysis indicated that toxin Phe^{24} contacted Asp^{402} in channel B chain, and Gly^{401} and His^{404} in channel C chain within a contact distance of 4 Å (Fig. 4C). In agreement with the experimental data (Fig. 3 and Table 1), the conserved Lys^{26} was found not to block channel pore, and just interacted with Asp^{402} and Met^{403} in channel B chain (Fig. 4D). Basically, these data indicated that BmKTX adopted a unique binding mode towards the potassium channel in the presence of Asp^{33} (Fig. 4). When toxin Asp^{33} was replaced by an histidine residue in BmKTX, this unique binding mode would be switched into the classical interaction mode for BmKTX–D33H analog which then uses its antiparallel β-sheet motif to recognize $K_v1.3$ (Fig. 4E). Completely different from the interaction details of Arg^{23}, Phe^{24} and Lys^{26} residues in

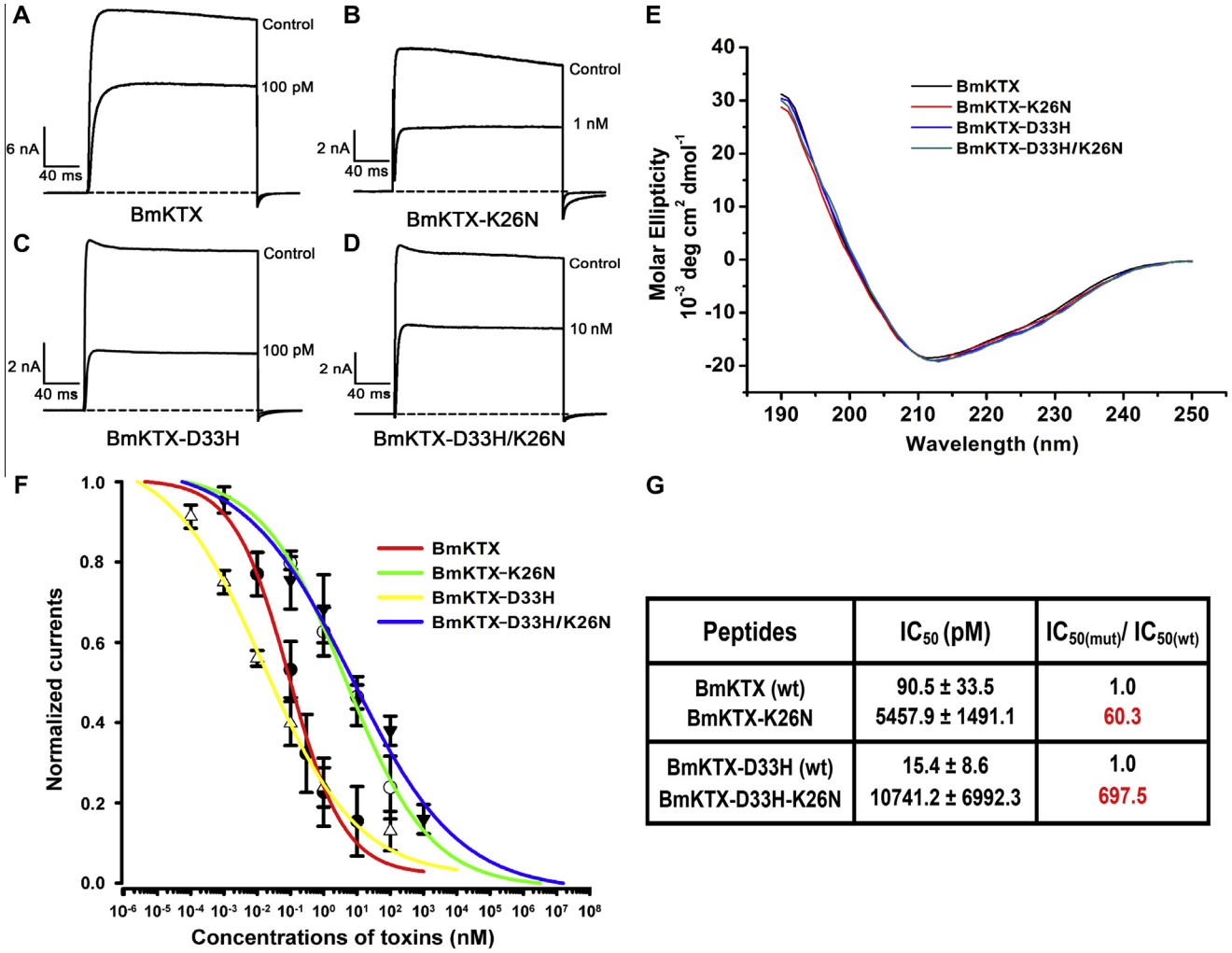

Peptides	IC_{50} (pM)	$IC_{50(mut)}/IC_{50(wt)}$
BmKTX (wt)	90.5 ± 33.5	1.0
BmKTX-K26N	5457.9 ± 1491.1	60.3
BmKTX-D33H (wt)	15.4 ± 8.6	1.0
BmKTX-D33H-K26N	10741.2 ± 6992.3	697.5

Fig. 3. Different roles of K26 residue in toxin BmKTX and BmKTX-D33H acting on Kv1.3 potassium channel. (A–D) Representative current traces of Kv1.3 showed the block of currents by BmKTX and its mutant peptides: (A) 100 pM BmKTX, (B) 1 nM BmKTX-K26N, (C) 100 pM BmKTX-D33H, (D) 10 nM BmKTX-D33H/K26N. (E) Circular dichroism spectra of BmKTX and its mutants. (F) Normalized Kv1.3 channel current inhibition by various concentrations of BmKTX and its mutants. (G) The IC_{50} values of BmKTX, BmKTX-D33H and their Lys26 mutants on Kv1.3 channel currents. Data represent mean ± S.E. of at least three experiments.

Table 1
Effect of BmKTX and its mutants in blocking Kv1.3 channels.

Peptides	IC_{50} (pM)	*n*	$IC_{50(mut)}/IC_{50(wt)}$
BmKTX	90.5 ± 33.5	5	1.0
N4A	437.3 ± 291.1	4	4.8
K6A	581.3 ± 148.5	4	6.4
K8A	410.5 ± 155.0	5	4.5
H9A	2140.6 ± 1026.4	5	23.6
Q12A	930 ± 330	5	10.3
K15A	55.7 ± 8.1	4	6.0
K18A	3898.7 ± 903.0	5	43.1
M22A	454.6 ± 131.2	4	5.0
R23A	175,706.7 ± 66,909.8	6	1940.5
F24A	9700 ± 3500	7	107.1
K26N	5457.9 ± 1491.1	5	60.3
K31A	821.2 ± 399.3	4	9.1
T35A	134.5 ± 61.4	5	1.5
P36A	1460.0 ± 424.8	4	16.1

Table 2
Effect of BmKTX-D33H and its mutants in blocking Kv1.3 channels.

Peptides	IC_{50} (pM)	*n*	$IC_{50(mut)}/IC_{50(wt)}$
BmKTX-D33H	15.4 ± 8.6	4	1.0
R23A	27,218.3 ± 8967.1	5	1770.6
F24A	20,998.1 ± 4161.3	4	1365.9
K26A	4555.8 ± 1556.7	4	295.8
I28A	721.9 ± 331.9	4	47.0
N29A	6164.6 ± 1499.2	4	401.0
H33A	430.9 ± 69.8	4	28.0
T35A	340.3 ± 195.2	4	22.1

BmKTX, the critical Arg^{23} of toxin BmKTX-D33H formed considerably strong interactions with Gly^{380}, Phe^{381}, Asp^{386} and Met^{403} in the C chain of $K_v1.3$ channel (Fig. 4F). In addition, the essential Phe^{24} was surrounded by a pocket formed by many nonpolar and polar residues (Phe^{381}, Asp^{402}, Met^{403}, His^{404} and Val^{406}) of $K_v1.3$ channel within a contact distance of 4 Å (Fig. 4G). Similar to the classical pore-blocking function of the conserved Lys^{26} in the highly homologous ADWX-1 peptide lacking Asp^{33} (Fig. 1) [13], Lys^{26} also plugged its side chain into the selectivity filter of $K_v1.3$ channel (Fig. 4H). Considering the amino acid sequence identities, but differential Asp^{33} residue between BmKTX and its analogs (Fig. 1), variation in the interaction modes with $K_v1.3$ channel highlighted the importance of Asp^{33} residue in mediating the novel BmKTX toxin–potassium channel interaction.

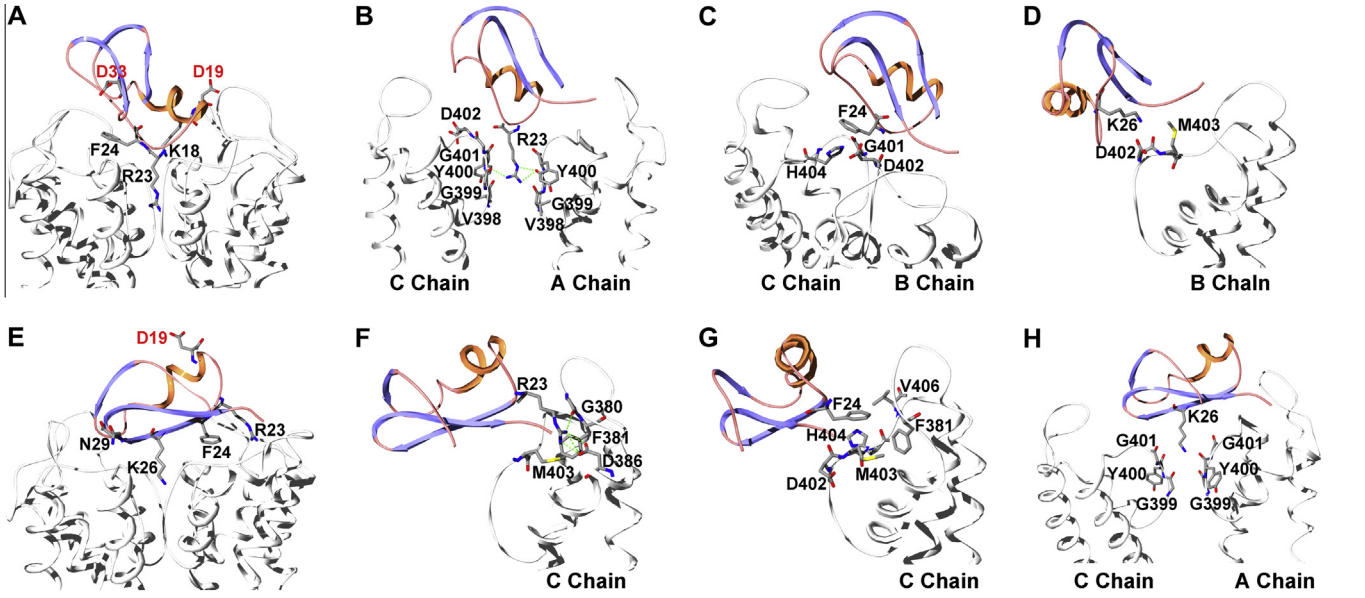

Fig. 4. Interaction of toxin BmKTX and BmKTX-D33H with Kv1.3 channel. (A) Interaction mode of BmKTX with K_v1.3 channel. BmKTX acidic residues and other key functional residues were marked. (B) Potassium channel pore-blocking Arg23 of BmKTX mainly contacted the conserved residues of K_v1.3 pore region. (C) Phe24 of BmKTX interacted with Asp402 in channel B chain, Gly401 and His404 in channel C chain. (D) Lys26 of BmKTX mainly contacted channel Asp402 and Met403. (E) Interaction mode of BmKTX-D33H with K_v1.3 channel. BmKTX-D33H acidic residues and other key functional residues were marked. (F) Arg23 of BmKTX-D33H was surrounded by residues from K_v1.3 pore and turret regions. (G) Phe24 of BmKTX-D33H was surrounded by residues from K_v1.3 pore and turret regions. (H) Potassium channel pore-blocking Lys26 of BmKTX-D33H mainly interacted with contacted the conserved residues of K_v1.3 pore region.

4. Discussion

Long-term molecular evolution of toxins produced by scorpions resulted in a great variety of potassium channel–blocking toxins. This variety in peptide sequences has been revealed by the extensive proteomic and transcriptomic analyses of animal venoms [12]. Different from the two classical interaction modes between scorpion toxins and potassium channels, the native scorpion toxin BmKTX was demonstrated to adopt a unique binding mode towards potassium channels in the presence of the Asp^{33} residue. Structurally, it made sense that toxin Asp^{33} plays a crucial role in defining the mode of binding of BmKTX towards K_v1.3 channel (Fig. S2). When the conserved Lys^{26} of BmKTX adopted the similar orientation to approach the selectivity filter of K_v1.3 channel as that of the homologous ADWX-1, BmKTX-D33H and ChTX toxins [5,6], there would be remarkably strong electrostatic repulsion occurring between toxin Asp^{33} and four conserved Asp^{402} residues in the pore region of K_v1.3 channel (Fig. S2A). These electrostatic repulsion forces would make scorpion toxin BmKTX gradually 'rotate' above the vestibule of K_v1.3 channel so that the conserved Lys^{26} leaves the axis of the channel selectivity filter and no longer plugs its side chain into the channel pore (Fig. S2A and S2B). Through the further synergetic electrostatic repulsion forces between two Asp residues of toxin BmKTX (Asp^{19} and Asp^{33}) and four Asp^{402} residues in the pore region of K_v1.3 channel, scorpion toxin BmKTX would accurately adjust its orientation above the vestibule of K_v1.3 channel and would use Arg^{23} instead to block the channel pore (Fig. S2C). Finally, BmKTX adopted the turn motif between the α-helix and the antiparallel β-sheet domains as the channel-interacting interface, and Arg^{23} instead of the conserved Lys^{26} as the new pore-blocking residue (Fig. S2D). Such a structural analysis well rationalizes the distinct binding modes between the highly similar BmKTX and BmKTX-D33H peptides (Figs. 1 and S1). Therefore, this study highlights the important role of toxin negatively charged residues in triggering various binding modes.

Acknowledgments

We thank Dr. Stephan Grissmer (University of Ulm, Ulm, Germany) for the gifts of K_v1.3 channel. This work was supported by grants from the National Basic Research Program of China (No. 2010CB529800), National High Technology Research and Development Program of China (2012AA020304), the National Natural Sciences Foundation of China (Nos. 30530140, 30973636, 31170789, 31200557 and 31000344), the New Century Excellent Talents in Wuhan University by the Ministry of Education of China (No. NCET-10-0651) and Wuhan City Science and Technology Foundation of China (No. 2013070204020046).

Appendix A. Supplementary data

Supplementary data associated with this article can be found, in the online version, at http://dx.doi.org/10.1016/j.bbrc.2014.03.101.

References

[1] J.A. Dunlop, C. Kamenz, G. Scholtz, Reinterpreting the morphology of the Jurassic scorpion Liassoscorpionides, Arthropod Struct. Dev. 36 (2007) 245–252.
[2] B.G. Fry, K. Roelants, D.E. Champagne, H. Scheib, J.D. Tyndall, G.F. King, T.J. Nevalainen, J.A. Norman, R.J. Lewis, R.S. Norton, C. Renjifo, R.C. de la Vega, The toxicogenomic multiverse: convergent recruitment of proteins into animal venoms, Annu. Rev. Genomics Hum. Genet. 10 (2009) 483–511.
[3] S. Mouhat, N. Andreotti, B. Jouirou, J.M. Sabatier, Animal toxins acting on voltage-gated potassium channels, Curr. Pharm. Des. 14 (2008) 2503–2518.
[4] S. Mouhat, B. Jouirou, A. Mosbah, M. De Waard, J.M. Sabatier, Diversity of folds in animal toxins acting on ion channels, Biochem. J. 378 (2004) 717–726.
[5] A. Banerjee, A. Lee, E. Campbell, R. Mackinnon, Structure of a pore-blocking toxin in complex with a eukaryotic voltage-dependent K^+ channel, Elife 2 (2013) e00594.
[6] S. Han, H. Yi, S.J. Yin, Z.Y. Chen, H. Liu, Z.J. Cao, Y.L. Wu, W.X. Li, Structural basis of a potent peptide inhibitor designed for Kv1.3 channel, a therapeutic target of autoimmune disease, J. Biol. Chem. 283 (2008) 19058–19065.
[7] M.L. Eriksson, B. Roux, Modeling the structure of agitoxin in complex with the Shaker K^+ channel: a computational approach based on experimental distance restraints extracted from thermodynamic mutant cycles, Biophys. J. 83 (2002) 2595–2609.

[8] H. Yi, S. Qiu, Z. Cao, Y. Wu, W. Li, Molecular basis of inhibitory peptide maurotoxin recognizing Kv1.2 channel explored by ZDOCK and molecular dynamic simulations, Proteins 70 (2008) 844–854.
[9] H. Yi, S. Qiu, Y. Wu, W. Li, B. Wang, Differential molecular information of maurotoxin peptide recognizing IKCa and Kv1.2 channels explored by computational simulation, BMC Struct. Biol. 11 (2011) 3.
[10] J. Feng, Y. Hu, H. Yi, S. Yin, S. Han, J. Hu, Z. Chen, W. Yang, Z. Cao, M. De Waard, J.M. Sabatier, W. Li, Y. Wu, Two conserved arginine residues from the SK3 potassium channel outer vestibule control selectivity of recognition by scorpion toxins, J. Biol. Chem. 288 (2013) 12544–12553.
[11] Y. Wu, Z. Cao, H. Yi, D. Jiang, X. Mao, H. Liu, W. Li, Simulation of the interaction between ScyTx and small conductance calcium-activated potassium channel by docking and MM-PBSA, Biophys. J. 87 (2004) 105–112.
[12] Z. Cao, Z. Di, Y. Wu, W. Li, Overview of scorpion species and their toxins from China, Toxins 6 (2014) 796–815.
[13] S. Han, S. Yin, H. Yi, S. Mouhat, S. Qiu, Z. Cao, J.M. Sabatier, Y. Wu, W. Li, Protein–protein recognition control by modulating electrostatic interactions, J. Proteome Res. 9 (2010) 3118–3125.
[14] R. Romi-Lebrun, B. Lebrun, M.F. Martin-Eauclaire, M. Ishiguro, P. Escoubas, F.Q. Wu, M. Hisada, O. Pongs, T. Nakajima, Purification, characterization, and synthesis of three novel toxins from the Chinese scorpion *Buthus martensi*, which act on K^+ channels, Biochemistry 36 (1997) 13473–13482.
[15] J.G. Renisio, R. Romi-Lebrun, E. Blanc, O. Bornet, T. Nakajima, H. Darbon, Solution structure of BmKTX, a K^+ blocker toxin from the Chinese scorpion *Buthus martensi*, Proteins 38 (2000) 70–78.
[16] R. Chen, W. Tong, J. Mintseris, L. Li, Z. Weng, ZDOCK predictions for the CAPRI challenge, Proteins 52 (2003) 68–73.
[17] D.A. Case, T.E. Cheatham 3rd, T. Darden, H. Gohlke, R. Luo, K.M. Merz Jr., A. Onufriev, C. Simmerling, B. Wang, R.J. Woods, The Amber biomolecular simulation programs, J. Comput. Chem. 26 (2005) 1668–1688.
[18] R.C. Rodriguez de la Vega, L.D. Possani, Current views on scorpion toxins specific for K^+-channels, Toxicon 43 (2004) 865–875.
[19] S.A. Goldstein, C. Miller, Mechanism of charybdotoxin block of a voltage-gated K^+ channel, Biophys. J. 65 (1993) 1613–1619.
[20] A. Gross, R. MacKinnon, Agitoxin footprinting the shaker potassium channel pore, Neuron 16 (1996) 399–406.
[21] V. Visan, Z. Fajloun, J.M. Sabatier, S. Grissmer, Mapping of maurotoxin binding sites on hKv1.2, hKv1.3, and hIKCa1 channels, Mol. Pharmacol. 66 (2004) 1103–1112.